

## Generation of magnetic-state polarization in light-induced collisional energy transfer: Weak-field, quasistatic-wing limit

P. R. Berman

*Department of Physics, New York University, 4 Washington Place, New York, New York 10003*

F. Schuller

*Laboratoire de Physique des Lasers, Université Paris-Nord, Avenue Jean-Baptiste Clément,  
93430 Villetaneuse, France*

G. Nienhuis

*Fysisch Laboratorium, Rijksuniversiteit Utrecht, Postbus 80 000, 3508 TA Utrecht, The Netherlands*

(Received 23 October 1989; revised manuscript received 20 February 1990)

A reaction of the form  $A_i + A'_i + \hbar\Omega \rightarrow A_f + A'_f$  has been referred to as light-induced collisional energy transfer (LICET). In such a reaction, atoms  $A$  and  $A'$  collide in the presence of a radiation field and absorb a photon during the collision, taking them from initial states  $(A_i, A'_i)$  to *different* final states  $(A_f, A'_f)$ . We calculate the final-state magnetic polarization produced in LICET for detunings  $\Delta = [(E_f + E_{f'}) - (E_i + E_i' + \hbar\Omega)]/\hbar$  in the quasistatic wing: that is, for  $|\Delta|\tau_c \gg 1$ , where  $\tau_c$  is the collision duration. Our results are compared with analogous depolarization rates for so-called "optical" collisions (reactions of the form  $A_i + A'_i + \hbar\Omega \rightarrow A_i + A'_f$ ). Similarities and differences between the LICET and "optical" collision theories are noted. Final-state LICET magnetic-state polarization is evaluated for a number of different  $A$ - $A'$  level schemes, assuming a dipole-dipole collisional interaction. Our results are shown to be in good agreement with experiment [A. Débarre, *J. Phys. B* **15**, 1693 (1982)].

### I. INTRODUCTION

A laser-assisted collision is one involving a combined collisional-radiative interaction. A typical laser-assisted collision can be written as a reaction of the form

$$A_I + \hbar\Omega \rightarrow A_F \quad (1.1)$$

where  $|I\rangle$  and  $|F\rangle$  are *composite* initial and final states, respectively, of atoms  $A$  and  $A'$  which are undergoing the collision, and  $\Omega$  is the frequency of the laser field that produces the transition from initial to final state. The eigenkets  $|I\rangle$  and  $|F\rangle$  may be expressed in terms of the individual atomic-state eigenkets as  $|I\rangle = |i\rangle|i'\rangle$ ,  $|F\rangle = |f\rangle|f'\rangle$ , where unprimed states refer to atom  $A$  and primed states refer to atom  $A'$ . Laser-assisted collisions have been classified into two broad categories. First, there are the so-called "optical" collisions<sup>1</sup> [or collisionally assisted radiative excitation<sup>2</sup> (CARE)] involving reactions of the form

$$A_i + A'_i + \hbar\Omega \rightarrow A_i + A'_f, \quad (1.2)$$

in which the state of atom  $A$  is unchanged. The transition from state  $i'$  to  $f'$  in atom  $A'$  is accompanied by the absorption of a photon of frequency  $\Omega$ , which is assumed to be nonresonant with the  $i'$ - $f'$  transition frequency. Consequently, the role of the collision is to provide or extract translational energy to compensate for the energy defect between the photon and transition frequencies. Second, there are the so-called "radiative" collisions<sup>3</sup> [or laser-induced collisional excitation transfer<sup>4</sup> (LICET) or

radiatively aided inelastic collisions<sup>2</sup> (RAIC)] involving reactions of the form

$$A_i + A'_i + \hbar\Omega \rightarrow A_f + A'_f \quad (1.3)$$

in which both atoms change their internal state. Any difference between the photon and (composite) initial to final state transition frequency can again be compensated by a corresponding change in the translational energy of the colliding atoms. Reviews of both CARE and LICET can be found in the literature.<sup>5</sup>

The initial thrust of experiment and theory involved a determination of the initial to final state cross sections.<sup>6</sup> It soon became appreciated, however, that additional information concerning the collisional interaction could be obtained by studying the final-state magnetic polarization produced in the reactions. The origin of the final-state polarization can be traced to the fact that excitation is produced by a laser field having a well-defined direction of incidence (and, often, a well-defined polarization). The laser field excitation leads to a polarized distribution of final-state Zeeman sublevels which is not totally destroyed during the collision. Such polarization effects have been studied extensively both theoretically<sup>7</sup> and experimentally<sup>8</sup> for CARE. On the other hand, polarization effects for LICET reactions have received limited attention. A theory of polarization effects was given for the impact core of the LICET profile<sup>9</sup> and a model (molecular) potential calculation of polarization effects for the entire line profile was presented by Julienne.<sup>10</sup> To our knowledge, there has been only one experiment in which the final state LICET polarization was measured.<sup>11</sup>

It is the purpose of this paper to develop further the theory of polarization effects in LICET. The general formalism that was presented in an earlier work<sup>9</sup> and applied to the impact line core is now applied to the so-called quasistatic wing of the LICET profile. The final-state LICET polarization that we obtain differs from that observed in CARE and can also differ from LICET polarization obtained by Julienne.<sup>10</sup> The reasons for these differences are discussed in terms of a simple physical picture describing the LICET process. Dramatic differences in final state polarizations are predicted for different LICET excitation schemes, which, at first glance, may seem quite similar. It is hoped that the predictions will serve as a stimulus for further experiments in this area.

In Sec. II, CARE and LICET are compared, neglecting effects of magnetic-state degeneracy. In this section, the notation is established and differences between CARE and LICET are discussed. In Sec. III, the results are generalized to include effects of magnetic-state degeneracy. Detailed calculations for depolarization in the quasistatic wing of the LICET profile are presented in Secs. IV and V, assuming a dipole-dipole collisional interaction. A "half-collision" picture of the excitation process<sup>7,8</sup> is used in Secs. III-V.

## II. CARE AND LICET—NEGLECT OF MAGNETIC STATE DEGENERACY

Both the CARE and LICET reactions are represented schematically by Eq. (1.1), in which a single photon of frequency  $\Omega$  from a field having amplitude  $\mathcal{E}$  is absorbed during a collision, taking the  $A$  and  $A'$  atoms from some initial composite state  $|I\rangle = |ii'\rangle$  to a final composite state  $|F\rangle = |ff'\rangle$ . To simplify the discussion somewhat, the following assumptions or approximations will be made throughout this paper. (i) LICET and CARE cross sections will be calculated to lowest nonvanishing order ( $\mathcal{E}^2$ ) of the applied radiation field. (ii) The field frequency is nearly equal to the composite frequency  $\omega_{FI}$  associated with the  $I \rightarrow F$  transition, such that  $|(\Omega - \omega_{FI})/(\Omega + \omega_{FI})| \ll 1$  (resonance or rotating-wave approximation). (iii) Any Doppler dephasing or atomic decay can be neglected on the time scale of the duration of a collision  $\tau_c$ . (iv) To insure that we are dealing with a collisionally assisted process (negligible transition amplitude in the absence of a collision), it is assumed that the laser field is turned on and off in a time that is long compared with the collision duration  $\tau_c$ . Moreover, for CARE, it is further assumed that the magnitude of the atom-field detuning  $\Delta$  defined by

$$\Delta = \Omega - \omega_{FI} \quad (2.1)$$

is larger than the Doppler width and any decay rate associated with the transitions, and that the applied field amplitude does not vary significantly in a time of order  $|\Delta|^{-1}$ . (v) the  $A-A'$  internuclear separation  $\mathbf{R}$  is calculated along a classical trajectory and can be considered as an explicit function of time. (vi) There is no collisional energy transfer in the absence of the applied radiation field.

Both CARE and LICET can be treated by a similar formalism. The Hamiltonian for the  $A-A'$  system in-

teracting with a radiation field is

$$H = H_0(\mathbf{r}) + H_c(\mathbf{r}, \mathbf{R}(t)) - \boldsymbol{\mu}_T \cdot \mathcal{E}(t), \quad (2.2)$$

where  $H_0$  is the sum of atomic Hamiltonians for atoms  $A$  and  $A'$ , ( $\mathbf{r}$  represents the electronic coordinates of either atom  $A$  or  $A'$ ),  $H_c(\mathbf{r}, \mathbf{R}(t))$  is the  $A-A'$  collisional Hamiltonian,  $\boldsymbol{\mu}_T = \boldsymbol{\mu} + \boldsymbol{\mu}'$  is the sum of dipole operators for atoms  $A$  and  $A'$ , and  $\mathcal{E}(t)$  is the applied field, assumed to be of the form

$$\mathcal{E}(t) = \frac{1}{2} (\mathcal{E}_0 e^{-i\Omega t} + \mathcal{E}_0^* e^{i\Omega t}), \quad (2.3)$$

where the field amplitude  $\mathcal{E}_0$  is taken to be constant during a collision.

It is sometimes convenient to expand the wave function as

$$|\Psi(t)\rangle = \sum_E a_E(t) |E(R)\rangle, \quad (2.4)$$

where  $|E(R)\rangle \equiv |E(R(t))\rangle$  is an instantaneous eigenket of  $[H_0 + H_c(R)]$ ; that is,

$$[H_0 + H_c(R)] |E(R)\rangle = E(R) |E(R)\rangle. \quad (2.5)$$

(The dependence of  $H_c$  on the direction of  $\mathbf{R}$  is suppressed in this section.) When Eq. (2.4) is substituted into the Schrödinger equation and Eq. (2.5) is used, one finds that the  $a_E(t)$  satisfy

$$i\hbar \dot{a}_E(t) = E(R) a_E(t) - \sum_{E'} \langle E(R) | \boldsymbol{\mu}_T | E'(R) \rangle \cdot \mathcal{E}(t) a_{E'}(t) - i\hbar \sum_{E' \neq E} \langle E(R) | \frac{d|E'(R)\rangle}{dt} a_{E'}(t). \quad (2.6)$$

It is to be noted that  $H_c(R) \sim 0$  as  $R \sim \infty$ ; consequently, the eigenkets  $|E(R)\rangle$  reduce to the composite state eigenkets  $|E\rangle = |ee'\rangle$  of  $H_0$  as  $R$  approaches infinity.

By assumption, collisions do not produce any transitions in the composite  $A-A'$  system in the absence of any radiation. Consequently, the last term in Eq. (2.6) can be dropped since it corresponds precisely to transitions of this nature. The resulting equation for  $a_E(t)$ ,

$$i\hbar \dot{a}_E(t) = E(R) a_E(t) - \sum_{E'} \langle E(R) | \boldsymbol{\mu}_T | E'(R) \rangle \cdot \mathcal{E}(t) a_{E'}(t), \quad (2.7)$$

can be given a simple interpretation in terms of a quasimolecular picture of the reaction. The  $A-A'$  system can be viewed as a quasimolecule with energy eigenvalues  $E(R)$  and corresponding eigenkets  $|E(R)\rangle$ . The field induces transitions between these quasimolecular states at a rate which depends on the dipole matrix element  $\langle E(R) | \boldsymbol{\mu}_T | E'(R) \rangle$ .

Within the context of the model, it is appropriate to approximate  $E(R)$  and  $|E(R)\rangle$  using time-independent perturbation theory on the Hamiltonian  $[H_0 + H_c(R)]$ . Labeling the eigenkets and eigenenergies of  $H_0$  by  $|E\rangle$  and  $E$ , respectively, it is an easy matter to show that

$$|E(R)\rangle \simeq |E\rangle + \sum_{E' \neq E} \frac{\langle E' | H_c(R) | E \rangle}{E - E'} |E'\rangle \quad (2.8a)$$

and

$$E(R) \simeq E + \hbar U_E(R), \quad (2.8b)$$

with

$$U_E(R) = \frac{1}{\hbar} \sum_{E' \neq E} \frac{|\langle E | H_c(R) | E' \rangle|^2}{E - E'}. \quad (2.9)$$

The quantity  $U_E(R)$  is the collisional frequency shift associated with level  $E$ . It is assumed implicitly that  $\langle E | H_c(R) | E \rangle = 0$ .

We are interested in the solution of Eq. (2.7) to lowest order in  $\mathcal{E}_0$ . If the atoms are in the state  $|I\rangle = |ii'\rangle$  at  $t = -\infty$ , then, in the resonance approximation and to lowest order in  $\mathcal{E}_0$ , the probability amplitude for the atoms to be in the state  $|F\rangle = |ff'\rangle$  at  $t = \infty$  is

$$|a_F(\infty)| = \left| \int_{-\infty}^{\infty} \chi_T(R(t)) \exp \left[ \frac{i}{\hbar} \int_0^t \Delta(R(t')) dt' \right] dt \right|, \quad (2.10)$$

where

$$\chi_T(R) = \frac{\langle F(R) | \mu_T | I(R) \rangle}{2\hbar} \cdot \mathcal{E}_0 \quad (2.11)$$

and

$$\Delta(R) = \Omega - \omega_{FI}(R), \quad (2.12)$$

with

$$\omega_{FI}(R) = F(R) - I(R). \quad (2.13a)$$

Note that one may also write

$$\omega_{FI}(R) = \omega_{FI} + U_{FI}(R), \quad (2.13b)$$

and

$$\Delta(R) = \Delta - U_{FI}(R), \quad (2.14)$$

where  $U_{FI}(R)$  is the radiative collisional frequency shift defined by

$$U_{FI}(R) = U_F(R) - U_I(R). \quad (2.15)$$

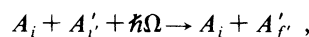
Equations (2.10)–(2.15) represent a formal solution to the CARE and LICET problems, neglecting effects of magnetic-state degeneracy. The LICET or CARE cross sections are defined as the value of  $|a_F(\infty)|^2$  averaged over the distribution of collision impact parameters and  $A$ - $A'$  relative speeds. The detailed structure of the profiles depends on the form of  $\chi(R)$  and  $U_{FI}(R)$ . However, in the line wings ( $|\Delta|\tau_c \gg 1$ ), the qualitative dependence of both the LICET and CARE cross sections on  $\Delta$  is similar. For ( $|\Delta|\tau_c \gg 1$ ), the magnitude of the CARE or LICET cross section depends critically on whether or not there are internuclear separations  $R$  for which  $\Delta(R)$ , as defined by Eq. (2.14), is equal to zero. Suppose for example, that the relative collisional shift  $U_{FI}(R)$  increases monotonically with decreasing  $R$ . Then, there are internuclear separations  $R$  for which  $\Delta(R) = 0$  if  $\Delta > 0$ , but none if  $\Delta < 0$ . Another way of stating this result is that the applied field can be resonant with the  $A$ - $A'$  quasimolecule for  $\Delta > 0$ , but not for  $\Delta < 0$  if  $U_{FI}(R) > 0$ . As a

consequence of this asymmetry, the RAIC and LICET cross sections possess a marked asymmetry for detunings  $|\Delta|\tau_c \gg 1$ . For the illustrative example given above, the *quasistatic wing* falls off as an inverse power of  $\Delta$  for  $\Delta > 0$ , while the *antistatic wing* falls off much more rapidly, exponentially with  $|\Delta|\tau_c$ . [If  $U_{FI}(R)$  decreases monotonically with decreasing  $R$ , the quasistatic wing occurs for  $\Delta < 0$  and the antistatic wing for  $\Delta > 0$ .] Experimental CARE and LICET profiles exhibit this asymmetric behavior.<sup>6</sup>

Although the molecular picture of excitation in the line wings is qualitatively similar for both CARE and LICET, there are some intrinsic differences between CARE and LICET that are particularly relevant to the present discussion. Consequently, it is helpful to examine the excitation mechanism a little more closely.

### A. CARE

A typical level scheme for the CARE reaction



in which  $|I\rangle = |ii'\rangle$ ,  $|F\rangle = |if'\rangle$ , is shown in Fig. 1. The corresponding quasimolecular energy level diagram is given in Fig. 2, assuming  $U_{FI}(R) > 0$ . We consider only the situation in which levels  $i'$  and  $f'$  have opposite parity, from which it follows from (2.8a) and (2.11) that the Rabi frequency

$$\begin{aligned} \chi_T(R) &\simeq \langle F | \mu_T | I \rangle \cdot \mathcal{E}_0 / 2\hbar \\ &= \langle f' | \mu' | i' \rangle \cdot \mathcal{E}_0 / 2\hbar \equiv \chi' \end{aligned} \quad (2.16)$$

is independent of  $R$  to lowest order in the collisional interaction. The corresponding CARE profile, calculated from Eq. (2.10), exhibits a  $\Delta^{-2}$  dependence for  $|\Delta|\tau_c \ll 1$  and a quasistatic-wing falloff that would vary as  $\Delta^{-(1+3/n)}$  for a collisional shift operator of the form  $U_{FI}(R) = C/R^n$ .

### B. LICET

A level scheme for the LICET reaction



is shown in Fig. 3. Since *both* atoms change their internal states, it follows immediately that

$$\langle I | \mu_T | F \rangle = \langle ii' | \mu + \mu' | ff' \rangle = 0. \quad (2.17)$$

Thus, in contrast to CARE, the Rabi frequency  $\chi_T(R)$

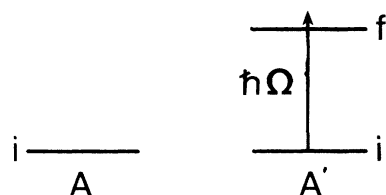


FIG. 1. Energy-level diagram for the CARE (collisionally aided radiative excitation) reaction  $A_i + A'_i + \hbar\Omega \rightarrow A_i + A'_i$ .

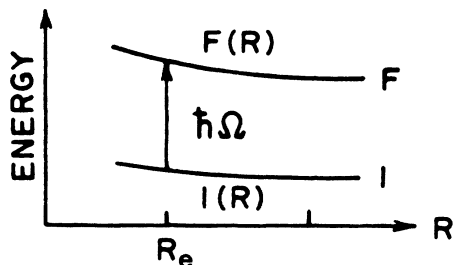


FIG. 2. Excitation scheme for the CARE reaction of Fig. 1 in the molecular-state picture. In the quasistatic wing, excitation occurs at an internuclear separation  $R = R_e$  for which  $\Omega = \omega_{FI}(R_e)$ .

given by Eqs. (2.11) and (2.8a) vanishes asymptotically as  $R \sim \infty$ . The combined radiative-collisional coupling  $\chi_T(R)$ , obtained from Eqs. (2.11) and (2.8a) is

$$\chi_T(R) = \frac{1}{2\hbar} \sum_E \left[ \frac{\langle F|\mu|E\rangle\langle E|H_c(R)|I\rangle \cdot \mathcal{E}_0}{\hbar\omega_{IE}} + \frac{\langle F|\mu'|E\rangle\langle E|H_c(R)|I\rangle \cdot \mathcal{E}_0}{\hbar\omega_{IE}} + \frac{\langle F|H_c(R)|E\rangle\langle E|\mu|I\rangle \cdot \mathcal{E}_0}{\hbar\omega_{FE}} + \frac{\langle F|H_c(R)|E\rangle\langle E|\mu'|I\rangle \cdot \mathcal{E}_0}{\hbar\omega_{FE}} \right]. \quad (2.18)$$

As has been discussed elsewhere,<sup>9</sup> the four terms appearing in Eq. (2.18), can be given a simple physical interpretation in the composite *atomic* basis according to the diagrams of Figs. 4(a)–4(d). In Fig. 4(a), the collision acts to produce a virtual intermediate state  $|E\rangle = |ef'\rangle$  and the field acts in atom  $A$  to complete the LICET transition to state  $|F\rangle = |ff'\rangle$ . In Fig. 4(b), the collision produces the virtual intermediate state  $|E\rangle = |fe'\rangle$  and the field acts on atom  $A'$  to complete the reaction. In Fig. 4(c), the field acts on atom  $A$  to produce virtual state  $|E\rangle = |ei'\rangle$  and the collision completes the reaction to final state  $|F\rangle = |ff'\rangle$ . In Fig. 4(d), the field acts on atom  $A'$  to produce virtual state  $|E\rangle = |ie'\rangle$ , and the collision completes the interaction.

The transition matrix element  $\chi_T(R)$  contains a sum

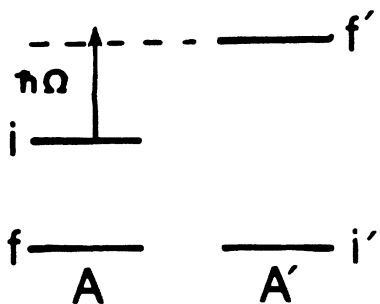


FIG. 3. Energy-level diagram for the LICET (light-induced collisional excitation transfer) reaction  $A_i + A'_i + \hbar\Omega \rightarrow A_f + A'_f$ .

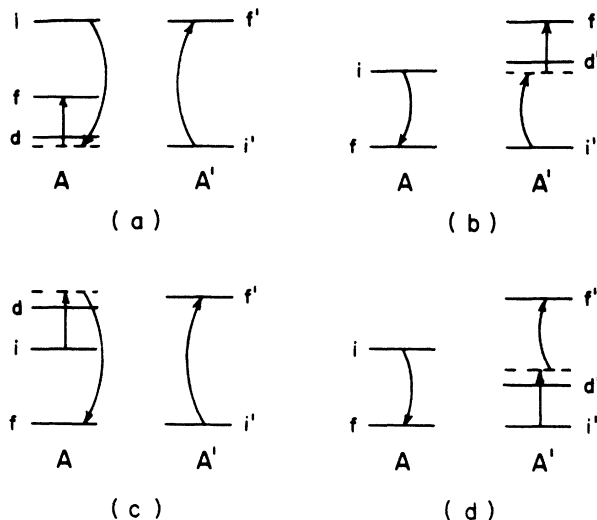


FIG. 4. Various LICET excitation schemes for the reaction  $A_i + A'_i + \hbar\Omega \rightarrow A_f + A'_f$ . The curved arrows represent the collisional coupling and the straight arrows the radiative coupling. The reactions proceed via an intermediate state which is nearly resonant with either the initial or final state. For (a), the intermediate state is  $|D\rangle = |df'\rangle$ ; for (b), it is  $|D\rangle = |fd'\rangle$ ; for (c), it is  $|D\rangle = |di'\rangle$ ; and for (d) it is  $|D\rangle = |id'\rangle$ .

over all intermediate states  $e$  and  $e'$  which enter the problem as virtual levels. However, as is often the case experimentally, there may be a “real” atomic level whose energy is nearly equal to that of the virtual state in atom  $A$  or  $A'$ . If one such level exists, its contribution to the sum in Eq. (2.18) is dominant, and the entire summation reduces to a single term. Nearly resonant intermediate levels are indicated by the solid lines labeled  $d$  or  $d'$  in Fig. 4. In our discussion of LICET, we always assume the existence of a nearly resonant intermediate state. Consequently, the summation in Eq. (2.18) reduces to a single term with intermediate state  $|E\rangle = |D_a\rangle = |df'\rangle$  [Fig. 4(a)],  $|E\rangle = |D_b\rangle = |fd'\rangle$  [Fig. 4(b)],  $|E\rangle = |D_c\rangle = |di'\rangle$  [Fig. 4(c)], or  $|E\rangle = |D_d\rangle = |id'\rangle$  [Fig. 4(d)]. Although the intermediate states are nearly-resonant and dominate the summation in (2.18), they still differ in energy sufficiently from the virtual energy levels [represented by the dashed lines in Fig. 4], to justify their virtual-state status. The population of state  $|D\rangle$  is negligibly small during and following the collision.<sup>12</sup>

In a quasimolecular picture, the existence of nearly resonant intermediate states affects the molecular energy levels as well as the transition rates. For Figs. 4(a) and 4(b), it is the initial-state energy  $I(R)$  which is seriously perturbed, whereas the final-state energy has no nearly resonant contributions. Explicitly, from (2.8), one finds

$$I(R) \simeq I + \frac{|\langle I|H_c(R)|D\rangle|^2}{\hbar\omega_{ID}}, \quad F(R) \simeq F;$$

$$|D\rangle = |df'\rangle, \quad (2.19a)$$

$$|D\rangle = |fd'\rangle. \quad (2.19b)$$

On the other hand, for Figs. 4(c) and 4(d), it is the final-

state energy  $F(R)$  which is strongly perturbed. One finds

$$F(R) \simeq F + \frac{|\langle F|H_c(\mathbf{R})|D \rangle|^2}{\hbar\omega_{FD}}, \quad I(R) \simeq I;$$

$$|D \rangle = |di' \rangle, \quad (2.19c)$$

$$|D \rangle = |id' \rangle. \quad (2.19d)$$

The molecular state diagrams corresponding to Figs. 4(a) and 4(b), and to 4(c) and 4(d) are drawn in Figs. 5(a) and 5(b), respectively. For the range of internuclear separations shown, it is assumed that variations in the energy of the weakly perturbed level are negligible.

In contrast to CARE, the LICET cross section varies as  $K_1 - K_2 \Delta^2$  for  $|\Delta| \tau_c \ll 1$ , where  $K_1$  and  $K_2$  are constants.<sup>9</sup> For a transition matrix element  $\chi_T(R)$  which varies as  $R^{-m}$  and a collisional shift that varies as  $R^{-n}$  ( $m, n > 3$ ) the quasistatic wing falls off as  $|\Delta|^{-[1+(3/n)-(2m/n)]}$ .

The qualitative nature of the total LICET cross section does not depend on the details of the excitation path. That is, independent of whether excitation is achieved via the nearly resonant level schemes of Figs. 4(a), 4(b), 4(c), or 4(d), the LICET profile is the same. When effects of magnetic-state degeneracy are taken into account, however, we will see that final-state magnetic coherence depends critically on the excitation path, yielding dramatically different results for Figs. 4(a)–4(d) (composite atomic basis) and for Figs. 5(a) and 5(b) (quasimolecular basis).

### III. CARE AND LICET CROSS SECTIONS, INCLUDING EFFECTS OF MAGNETIC DEGENERACY

The discussion of Sec. II is now extended to include effects related to the magnetic degeneracy of the atomic levels. In particular, we wish to calculate a quantity  $P$  defined by

$$P = \frac{S_z - S_x}{S_z + S_x}, \quad (3.1)$$

where  $S_\alpha$  ( $\alpha = x, z$ ) is the intensity of fluorescence polarized in the  $\alpha$  direction emitted from final state  $f'$  of atom  $A'$  following CARE or LICET excitation. It is assumed that the *incident* field participating in the CARE or LICET reaction is linearly polarized in the  $z$  direction

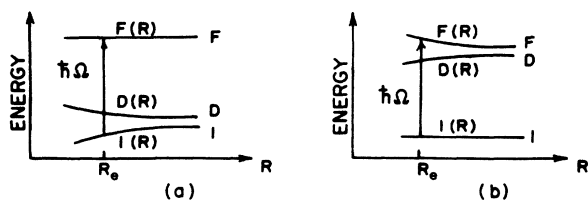


FIG. 5. Quasimolecular energy levels as a function of  $A-A'$  internuclear separation  $R$ . The asymptotic values  $I$  and  $F$  are the energies of the composite atomic states. (a) corresponds to the LICET excitation schemes of Figs. 4(a) and 4(b) while (b) corresponds to that of Figs. 4(c) and 4(d). For the frequency shown, the  $I(R) \rightarrow F(R)$  transition is resonant at  $R = R_e$ .

and is incident in the  $y$  direction. This field can give rise to a final-state magnetic polarization which is only partially destroyed in the collisional-radiative excitation process. As such, the final-state polarization, monitored through the ratio  $P$ , serves as a measure of the collisional interaction, providing significantly more information than *total* cross section data alone.<sup>7-10</sup>

The ratio  $P$  can be related directly to final-state reduced density matrix elements for atom  $A'$ . In other words, one must calculate the final state distribution of magnetic sublevel population and coherence in atom  $A'$  to determine the polarization ratio  $P$ . To achieve this goal, the calculation of Sec. II must be modified to include effects arising from magnetic state degeneracy. Each state of the composite atomic basis is now labeled  $|Emm' \rangle = |em \rangle |e'm' \rangle$ . For a given total angular momenta  $j_e$  and  $j_{e'}$  of levels  $e$  and  $e'$ , respectively, the state  $|E \rangle$  is  $(2j_e + 1)(2j_{e'} + 1)$ -fold degenerate. Collisions can mix these degenerate sublevels even in the absence of any applied fields. It turns out to be convenient to use a coupled basis in the composite atomic basis defined by

$$|EJ_E M \rangle = \sum_{mm'} C(j_e, j_{e'}, J_E; m, m', M) |e_j_e m \rangle |e'_{j_{e'}} m' \rangle, \quad (3.2)$$

where  $C(j_1, j_2, j_3; m_1, m_2, m_3)$  is a Clebsch-Gordan coefficient and  $J_E$  varies from  $|j_e - j_{e'}|$  to  $(j_e + j_{e'})$ .

It is sometimes convenient to use a molecular basis rather than the composite atomic basis. As in Sec. II, molecular state eigenkets are defined as eigenkets of  $H_0 + H_c(\mathbf{R}(t))$ , i.e.,

$$[H_0 + H_c(\mathbf{R}(t))] |E; \Lambda_E, M_{\Lambda_E}; t \rangle = \Lambda_E(t) |E; \Lambda_E, M_{\Lambda_E}; t \rangle. \quad (3.3)$$

The eigenkets are labeled as follows:  $E$  refers to the  $(2j_e + 1)(2j_{e'} + 1)$  manifold of levels,  $\Lambda_E$  is the energy of the state,  $M_{\Lambda_E}$  distinguishes among degenerate states having the same  $\Lambda_E$ , and  $t$  is a reminder that these eigenkets are a function of the interatomic separation  $\mathbf{R}(t)$ . As  $R \sim \infty$ , the eigenket  $|E; \Lambda_E, M_{\Lambda_E}; \pm \infty \rangle$  goes over into a *linear superposition* of eigenkets  $|EJ_E M_E \rangle$ . We will employ a shorthand notation in which a label  $E$  stands for  $(E; \Lambda_E, M_{\Lambda_E})$  and a label  $E'$  for  $(E; \Lambda'_E, M'_{\Lambda'_E})$  ( $E$  and  $E'$  are in the same manifold). In this notation, a sum over  $E$  represents a sum over  $\Lambda_E$  and  $M_{\Lambda_E}$  *within* the  $E$  manifold of levels.

The generalization of the calculation of Sec. II to include effects of magnetic degeneracy is straightforward. The resulting equations must be solved numerically in the most general case. In the quasistatic wing of the profile, however, it has been shown that there is some justification for using a "half-collision" picture of the excitation process, for which analytical results can be obtained.<sup>7,13</sup> The basic ingredients of such a theory which are relevant to the present discussion are outlined below. Details of the calculations may be found in Refs. 7, 9, and 13.

The collision is basically broken down into two spatial regions. A decoupling radius  $R_w = R(\pm t_d)$  is introduced ( $R_w$  is approximately equal to the so-called Weisskopf radius of pressure broadening theory and is of order 0.5 nm) such that, for  $A-A'$  internuclear separations  $R < R_w$ , the molecular states form a "good" adiabatic basis. On the other hand, for  $R > R_w$ , the collisional interaction is assumed to be sufficiently weak to allow one to neglect all effects of depolarization in this region.<sup>13,14</sup> For a given detuning in the quasistatic wing, CARE or LICET excitation occurs for internuclear separations  $R_e = R(t_e)$  such that

$$\Omega = \omega_{FI}(R_e) = \Lambda_F(t_e) - \Lambda_I(t_e), \quad (3.4)$$

that is, for molecular transition frequencies equal to the incident laser frequency.

$$\begin{aligned} \sigma_{KQ}^{J_F J'_F} = & 2N_I^{-1} \sum_{R_e} \sum_{\tilde{M}, \tilde{M}'} S_{\Lambda_F \Lambda_I}(R_e) (2K+1)^{-1} G_{KQ} (-1)^{\tilde{Q}} (-1)^{J'_F - M'_{\Lambda'_F}} B(\Lambda_F, M_{\Lambda_F}, J_F) B(\Lambda_F, M'_{\Lambda'_F}, J'_F)^* \\ & \times C(1, 1, K; \tilde{M}, \tilde{M}', -\tilde{Q}) C(J_F, J'_F, K; M_{\Lambda_F}, -M'_{\Lambda'_F}, Q') \\ & \times \langle d_{QQ}^K(\varphi - \theta) \rangle \langle F; t_e | (-1)^{\tilde{M}} (\tilde{\mu}_T)_{-\tilde{M}} | I; t_e \rangle \langle I; t_e | (-1)^{\tilde{M}'} (\tilde{\mu}_T)_{-\tilde{M}'} | F'; t_e \rangle \delta_{\Lambda_F \Lambda'_F}. \end{aligned} \quad (3.5)$$

The symbols appearing in this equation are defined as follows. The quantity  $\sigma_{KQ}^{J_F J'_F}$  is the cross section for excitation of density matrix element  $\rho_{KQ}^{J_F J'_F}$ , written in an irreducible tensor basis. The quantity  $N_I = (2j_i + 1)(2j_{i'} + 1)$  is the total number of sublevels in the initial-state manifold. The quantity  $S_{\Lambda_F \Lambda_I}(R_e)$  is given by

$$\begin{aligned} S_{\Lambda_F \Lambda_I}(R_e) = & \pi^2 \hbar^{-2} v_r^{-1} [R_{\Lambda_F \Lambda_I}(t_e)]^2 \\ & \times |d\omega_{\Lambda_F \Lambda_I} / dR_{\Lambda_F \Lambda_I}(t_e)|^{-1}, \end{aligned} \quad (3.6)$$

where  $v_r$  is the  $A-A'$  relative speed. The factor  $G_{KQ}$  is defined as

$$G_{KQ} = \sum_{MM'} (-1)^Q C(1, 1, K; M, M', -Q) \mathcal{E}_0^M (\mathcal{E}_0^*)^{M'}, \quad (3.7)$$

where  $\mathcal{E}_0^M$  is a spherical component of the laser-field amplitude  $\mathcal{E}_0$  (expressed in the laboratory frame). The quantity  $B(\Lambda_F, M_{\Lambda_F}, J_F)$  is a coefficient that relates the molecular basis eigenkets

$$|F; t\rangle = |F; \Lambda_F, M_{\Lambda_F}; t\rangle \quad (3.8)$$

to the composite state eigenkets  $|FJ_F M_F; t\rangle$  in a system quantized along the internuclear axis at time  $t$  via

$$|F; t\rangle = \sum_{J_F M_F} B(\Lambda_F, M_{\Lambda_F}, J'_F) |FJ_F M_F; t\rangle \delta_{M_F M_{\Lambda_F}}. \quad (3.9)$$

The quantity

$$\langle d_{QQ}^K(\varphi - \theta) \rangle = \langle \mathcal{D}_{QQ}^{(K)}(0, \varphi - \theta, 0) \rangle,$$

where  $\mathcal{D}^{(K)}$  is a rotation matrix, is given by

A "half-collision" picture emerges in which excitation occurs at one or more internuclear separations for a given frequency. Following excitation, the rotation of the molecular axis during the collision produces phase changes in each of the molecular states. The phase changes in the molecular basis correspond to depolarization in the composite atomic basis. The depolarization continues until an internuclear separation  $R = R_w$  is reached, after which no further depolarization occurs. This picture has been very useful in explaining CARE depolarization in the quasistatic wing.<sup>7,8,13</sup>

Assuming that atoms  $A$  and  $A'$  enter the collision in an initially unpolarized state, one finds that the cross sections for CARE or LICET excitation in the quasistatic wing, suitably averaged for all collision orientations and impact parameters is given by

$$\langle d_{QQ}^K(\varphi - \theta) \rangle = \frac{1}{2} \int_{-\pi/2}^{\pi/2} \cos\theta d_{QQ}^K(\varphi - \theta) d\theta. \quad (3.10)$$

The angle  $\theta$  is the angle between the impact parameter  $\mathbf{b}$  and  $\mathbf{R}_e$ , while  $\varphi$  is the angle between  $\mathbf{b}_e$  and  $\mathbf{R}(t_d)$  [i.e.,  $(\varphi - \theta)$  is the rotation angle of the internuclear axis between excitation and "decoupling"]. The quantity  $(\tilde{\mu}_T)_M$  is a component of the total dipole moment operator expressed in a spherical basis in a system of coordinates quantized along the internuclear axis at the time of excitation.

Equation (3.5) is a general result for CARE or LICET excited-state cross sections in the coupled angular-momenta composite atomic basis, assuming that the initial state is unpolarized and that collisions occur along straight-line paths. It was derived using the method of stationary phase, neglecting any terms arising from the interference of different excitation channels  $t_e$ .<sup>13</sup> Furthermore, all depolarization beyond a decoupling radius  $R_w = R(t_d)$  was assumed to be negligible; the radius  $R(t_d)$  was chosen to coincide with the maximum internuclear separation for which the adiabatic molecular basis is a "good" basis [generalization of the results to allow for depolarization for  $R > R(t_d)$  is easily incorporated into the formalism if desired]. All matrix elements are now written in the molecular basis  $|E; \Lambda_E, M_{\Lambda_E}; t_e\rangle$  which are related via the coefficients  $B(\Lambda, M_{\Lambda}, J_E)$  of Eq. (3.9) to the composite atomic basis eigenkets  $|EJ_E M_{J_E}; t_e\rangle$  in a system quantized along the internuclear axis at the time of excitation. Equation (3.5) can be traced over states of atom  $A$  to get cross sections for excitation of atom  $A'$  in an irreducible tensor basis.<sup>9</sup>

Although Eq. (3.5) applies to both CARE and LICET excitation, there are qualitative differences in the polar-

izations produced in the two types of reactions. These differences are linked to the fact that the coupling from initial to final state involves an  $R$ -dependent matrix element for LICET but not for CARE. Moreover, the LICET excitation schemes employ a nearly resonant intermediate state which strongly influences the structure of the coupling. As a result, the polarization produced at excitation depends critically on which of the excitation schemes of Fig. 4 is applicable. For example, owing to near-resonant enhancement involving the *initial*-state manifold in Figs. 4(a) and 4(b), the final-state manifold of levels is not significantly perturbed at the excitation radius  $R_e$ . Consequently, depolarization following excitation can be neglected for the excitation schemes of Figs. 4(a) and 4(b). A similar situation does not arise in CARE.

#### IV. SPECIFIC EVALUATION OF THE CROSS SECTIONS

Equation (3.5) is now evaluated for the various LICET excitation schemes of Fig. 4, assuming a dipole-dipole collisional interaction between atoms  $A$  and  $A'$ . All molecular eigenstates in the initial- and final-state manifolds will be calculated to first order in the collisional interaction  $H_c(\mathbf{R})$ , while the molecular state eigenenergies will be calculated to second order in  $H_c(\mathbf{R})$ .

Approximate values for the eigenkets and eigenvalues can be obtained from Eq. (3.3). In a given manifold  $E$ , the energy levels of  $H_0$  appearing in Eq. (3.3) are degenerate. To remove this degeneracy, one must go to second order in the perturbation  $H_c(\mathbf{R})$ .<sup>5</sup> To carry out this procedure,<sup>15</sup> it is necessary to diagonalize the Hamiltonian

$$H_0 + \sum_{J_D M_D} \frac{H_c(\mathbf{R}(t_e)) |DJ_D M_D\rangle \langle DJ_D M_D| H_c(\mathbf{R}(t_e))}{\hbar\omega_{ED}}, \quad E = I, F$$

where  $D$  is any of the intermediate-state manifolds shown in Fig. 4. If one diagonalizes this Hamiltonian, he obtains eigenkets  $|E; t_e\rangle^{(0)}$  which are correct to zeroth order in  $H_c$  and eigenenergies  $\Lambda_E(t_e)$  which are correct to second order in  $H_c$ . It is convenient to carry out this diagonalization using the composite atomic state basis eigenkets  $|E J_E M_E; t_e\rangle$ . The dipole-dipole interaction takes on the particularly simple form in this coupled angular-momenta basis given by<sup>16</sup>

$$H_c(\mathbf{R}(t_e)) = -\frac{4\pi}{(R(t_e))^3} \left(\frac{2}{3}\right)^{1/2} V_{20}(1, 1; t_e), \quad (4.1)$$

where  $V_{20}(1, 1; t_e)$  is an irreducible tensor operator

$$V_{20}(1, 1; t_e) = \sum_{q, q'} C(1, 1, 2; q, q', 0) T_{1q}(A, t_e) T_{1q'}(A', t_e) \quad (4.2)$$

and  $T_{1q}(A, t_e)$  and  $T_{1q'}(A', t_e)$  are irreducible tensor operators associated with atoms  $A$  and  $A'$ , respectively, expressed in terms of basis eigenkets quantized along the internuclear axis at the times of excitation. Consequently, we are left with the problem of diagonalizing submatrices in the initial- and final-state manifolds having matrix elements given by

$$E \delta_{J_E J'_E} \delta_{M_E M'_E} + \sum_{J_D} \frac{32\pi^2}{3(R(t_e))^6} \frac{\langle E J_E M_E; t_e | V_{20}(1, 1, t_e) | D J_D M_D; t_e \rangle \langle D J_D M_D; t_e | V_{20}(1, 1, t_e) | E J'_E M'_E; t_e \rangle \delta_{M_E M'_E}}{\hbar\omega_{ED}}, \quad E = I, F. \quad (4.3)$$

As is implicit in Eq. (3.9), the molecular-state eigenkets are not necessarily identical to the internuclear basis eigenkets. This is seen explicitly in expression (4.3); although the submatrix is diagonal in the magnetic index  $M_E$ , it need not be diagonal in  $J_E$ . The  $B(\Lambda, M_\Lambda, J)$  of Eq. (3.9) are chosen in a manner to produce molecular-state eigenkets  $|E; \Lambda_E, M_{\Lambda_E}; t_e\rangle^{(0)}$  which diagonalize the submatrix (4.3). In the specific examples to be considered below, we ultimately choose a final state for which the angular momentum of atom  $A$  is equal to zero,  $j_f = 0$ . In that case, there is only a single value  $J_F = j_{f'}$  (the final-state angular momentum of atom  $A'$ ) for the composite-state coupled angular momentum. Since  $J_F = J'_F = j_{f'}$  in expression (4.3), it follows that, in the *final-state* manifold, the molecular eigenkets are identical with the internuclear basis ones, i.e.,

$$|F; t_e\rangle^{(0)} \equiv |F j_{f'} m_{f'}; t_e\rangle, \quad j_f = 0; \quad (4.4a)$$

$$B(\Lambda_F, M_{\Lambda_F}, J_F) = \delta_{J_F j_{f'}}, \quad j_f = 0. \quad (4.4b)$$

In addition, the cross section (3.5) is written directly in terms of atom  $A'$  coordinates as

$$\sigma_{KQ}^{J_F J'_F} \rightarrow (\sigma'_{k'q'})^{j_{f'} j_{f'}} \equiv \sigma'_{k'q'}(j_{f'}), \quad j_f = 0. \quad (4.4c)$$

The explicit expressions for the cross section depend on which of the excitation schemes of Fig. 4 is used. In each case, a single, nearly resonant, composite intermediate-state manifold  $|D J_D M_D; t_e\rangle$  enters the calculation. These states are not seen explicitly in Eq. (3.5), but are contained implicitly in the molecular-state eigenkets. The matrix elements  $\langle I; t_e | (\bar{\mu}_T)_{\bar{M}} | F; t_e \rangle$  needed in Eq. (3.5) vanish for LICET if the zeroth-order eigenkets are used (they would not vanish for CARE). Consequently, it is necessary to go to first order in  $H_c(\mathbf{R})$  and use the eigenkets obtained by perturbation theory

$$|E; t_e\rangle^{(1)} = |E; t_e\rangle^{(0)} + \sum_{J_D M_D} \frac{\langle DJ_D M_D; t_e | H_c(\mathbf{R}(t_e)) | E; t_e \rangle^{(0)} | DJ_D M_D; t_e \rangle}{\hbar\omega_{ED}}, \quad E = I, F \quad (4.5)$$

where  $H_c(\mathbf{R})$  is given by (4.1).

#### A. Excitation schemes of Figs. 4(a) and 4(b)

For the excitation schemes of Figs. 4(a) and 4(b), the final-state collisional interaction can be neglected. The eigenenergies are given by expressions analogous to those in Eq. (2.19a) and (2.19b):

$$\Lambda_F(t, \alpha) = F, \quad (4.6)$$

$$\Lambda_I(t, \alpha) = I + \sum_{J_D M_D} \frac{|^{(0)}\langle I; t | H_c(\mathbf{R}(t_e)) | D_\alpha J_D M_D; t \rangle|^2}{\hbar\omega_{ID_\alpha}}, \quad \alpha = a, b$$

where  $\alpha = a, b$  labels the excitation scheme of Fig. 4 (recall that  $F$  and  $I$  refer to the unperturbed final and initial-state energies, respectively). The corresponding eigenkets are given by

$$|F; t_e; \alpha\rangle \simeq |F J_F M_F; t_e\rangle, \quad (4.7a)$$

$$|I; t_e; \alpha\rangle \simeq |I; t_e\rangle^{(0)} + \sum_{J_D M_D} \frac{\langle D_\alpha J_D M_D; t_e | H_c(\mathbf{R}(t_e)) | I; t_e \rangle^{(0)} | D_\alpha J_D M_D; t_e \rangle}{\hbar\omega_{ID_\alpha}}, \quad \alpha = a, b. \quad (4.7b)$$

From Eqs. (4.7a) and (3.9), it follows that the  $B(\Lambda_F, M_{\Lambda_F}, J)$  in Eq. (3.5) are equal to unity. Furthermore, since the final-state collisional interaction is negligible, there is no depolarization following excitation and one can set  $\varphi = \theta$  and

$$d_{\hat{Q}\hat{Q}'}^k(0) = \delta_{\hat{Q}\hat{Q}'}, \quad (4.8)$$

in Eq. (3.5).

When Eqs. (4.6)–(4.8) are substituted into Eq. (3.5) and some sums over magnetic substates are carried out, one finds an excitation cross section:

$$\sigma_{KQ}^{J_F J'_F}(\alpha) = 2N_I^{-1} \sum_{R_e} \sum_{I, J_D} S_{F\Lambda_I}(R_e) (2J_D + 1)^{-1} (-1)^{J'_F - J_D} \langle D_\alpha J_D || \mu_T || F J'_F \rangle \langle D_\alpha J_D || \mu_T || F J_F \rangle^* G_{KQ} \times \left\{ \begin{matrix} 1 & J_F & J_D \\ J'_F & 1 & K \end{matrix} \right\} \frac{|^{(0)}\langle I; t_e | H_c(\mathbf{R}(t_e)) | D_\alpha J_D M_D; t_e \rangle|^2}{(\hbar\omega_{ID_\alpha})^2}, \quad \alpha = a, b, \quad (4.9)$$

where  $\langle \dots || \dots || \dots \rangle$  is a reduced matrix element and  $\left\{ \begin{matrix} \dots \\ \dots \end{matrix} \right\}$  is a  $(6-J)$  symbol.<sup>17</sup>

If  $j_f = 0$ , then Eq. (4.9) can be simplified. For the dipole-dipole interaction (4.1) and  $j_f = 0$ , one finds an excitation cross section

$$\sigma'_{k'q'}(j_f; \alpha) = \frac{64\pi^2}{3} N_I^{-1} (\hbar\omega_{ID_\alpha})^{-2} \times \sum_{R_e} \sum_{\Lambda_I, M_{\Lambda_I}} R_{F\Lambda_I}^{-6}(t_e) S_{F\Lambda_I}(R_e) G_{k'q'} \times (2J_D + 1)^{-2} \langle D_\alpha J_D || V^{(2)}(1, 1) || I J_I \rangle \langle D_\alpha J_D || V^{(2)}(1, 1) || I J'_I \rangle^* \times |\langle D_\alpha J_D || \mu_T || F j_f \rangle|^2 (-1)^{j_f - J_D} B(\Lambda_I, M_{\Lambda_I}, J_I) B^*(\Lambda_I, M_{\Lambda_I}, J'_I) \times \left\{ \begin{matrix} 1 & j_f & J_D \\ j_f & 1 & k' \end{matrix} \right\} C(J_I, 2, J_D; M_{\Lambda_I}, 0, M_{\Lambda_I}) C(J'_I, 2, J_D; M_{\Lambda_I}, 0, M_{\Lambda_I}), \quad \alpha = a, b, \quad (4.10)$$

where an equation analogous to (3.9) has been used for the initial-state eigenkets. We now consider some explicit values for  $j_i, j'_i, j_d, j'_d, j_f$ , and  $j'_f$ . All excitation schemes refer to Fig. 4.

Excitation scheme a:  $j_i = j'_i = 0, j_d = j'_d = 1, j_f = 0,$

$j'_f = 1$ . For this level scheme,  $J_I = 0$  so that the only intermediate state which enters has  $J_D = 2$  [otherwise the reduced matrix element in (4.10) vanishes]. The nondegenerate initial-state [see Fig. 6(a)] has an energy calculated from Eq. (4.6) equal to

$$\Lambda_I(R, a) = I - C_a / R^6, \quad (4.11a)$$

where

$$C_a = \frac{32\pi^2}{3} \frac{|\langle I0 || V^{(2)}(1,1) || D2 \rangle|^2}{\hbar\omega_{D_a I}}. \quad (4.11b)$$

Using Eqs. (4.6), (4.11), (3.4), (2.12), (2.1), and (3.6) in Eq. (4.10), one finds an excitation cross section

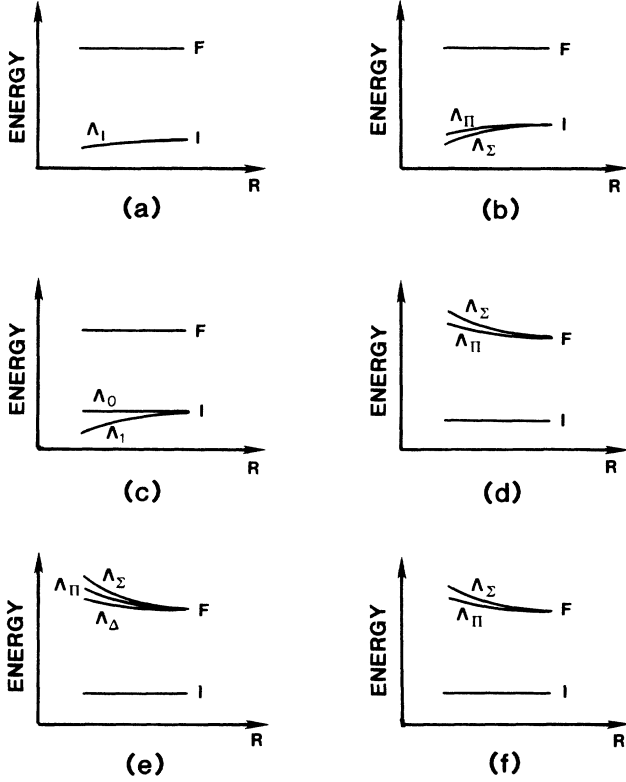


FIG. 6. Molecular energy-level diagrams for the six cases discussed in the text. (a) excitation scheme *a* (from Fig. 4):  $j_i=j_{i'}=0, j_d=j_{d'}=1, j_f=0, j_{f'}=0, J_I=0, J_F=1$ . The final level is three-fold degenerate. (b) excitation scheme *b* (from Fig. 4):  $j_i=1, j_{i'}=0, j_d=0, j_{d'}=1, j_f=0, j_{f'}=2, J_I=1, J_F=2$ . The  $\Lambda_{II}$  level is two-fold degenerate and level *F* is five-fold degenerate. (c) excitation scheme *b* (from Fig. 4):  $j_i=j_{i'}=1, j_d=j_{d'}=0, j_f=0, j_{f'}=1, J_I=0, 1, 2; J_F=1$ . Only the state having  $J_I=2, M_I=0$  (labeled  $\Lambda_1$ ) has its energy modified by the collisional interaction. The level labeled  $\Lambda_0$  is eight-fold degenerate and level *F* is three-fold degenerate. (d) excitation scheme *c* (from Fig. 4):  $j_i=j_{i'}=0, j_d=1, j_{d'}=0, j_f=0, j_{f'}=1, J_I=0, J_F=1$ . Level  $\Lambda_{II}$  is two-fold degenerate. (e) excitation scheme *d* (from Fig. 4):  $j_i=1, j_{i'}=0, j_d=j_{d'}=1, j_f=0, j_{f'}=2, J_I=1, J_F=2$ . Level *I* is three-fold degenerate and levels  $\Lambda_{II}$  and  $\Lambda_{\Delta}$  are each two-fold degenerate. (f) excitation scheme *d* (from Fig. 4):  $j_i=j_{i'}=1, j_d=1, j_{d'}=0, j_f=0, j_{f'}=1, J_I=0, 1, 2; J_F=1$ . Level *I* is nine-fold degenerate and level  $\Lambda_{II}$  is two-fold degenerate. Note that for the level schemes of Figs. 4(a) and 4(b) that  $\omega_{DI} > 0$  and for those of Figs. 4(c) and 4(d) that  $\omega_{DF} < 0$ . The sign of  $\omega_{DI}$  and  $\omega_{DF}$  determines the relative sign of the collisional shift of levels *I* and *F*, respectively.

$$\begin{aligned} \sigma'_{k'q'}(1, a) = & \frac{-32\pi^4(\hbar\omega_{ID_a})^{-2}}{9\hbar^3/2v_r|C_a|^{1/2}|\Delta|^{1/2}} G_{k'q'}(\frac{1}{25}) \\ & \times |\langle D_a 2 || V^{(2)}(1,1) || I0 \rangle|^2 \\ & \times |\langle D_a 2 || \mu || F1 \rangle|^2 \begin{Bmatrix} 1 & 1 & 2 \\ 1 & 1 & k' \end{Bmatrix}, \end{aligned} \quad (4.12)$$

where  $G_{kq}$  is given by (3.7) and  $\Delta = \Omega - \omega_{FI}$  is the detuning.

*Excitation scheme b:*  $j_i=1, j_{i'}=0, j_d=0, j_{d'}=1, j_f=0, j_{f'}=2$ . For this level scheme  $J_I=J_D=1$  and the zeroth-order initial state eigenkets [obtained from (4.3)] are given by

$$\begin{aligned} |I; \Sigma, 0; t_e \rangle^{(0)} &= |I; J_I=1, M_I=0; t_e \rangle, \\ |I; \Pi, \pm 1; t_e \rangle^{(0)} &= |I; J_I=1, M_I=\pm 1; t_e \rangle, \end{aligned} \quad (4.13)$$

along with the corresponding eigenenergies

$$\begin{aligned} \Lambda_{\Sigma}(R, b) &= I - C_{b\Sigma} / R^6, \\ \Lambda_{\Pi}(R, b) &= I - C_{b\Pi} / R^6, \end{aligned} \quad (4.14)$$

where

$$\begin{aligned} C_{b\Sigma} &= C^2(1, 2, 1; 0, 0, 0) \bar{C}_b = \frac{2}{3} \bar{C}_b, \\ C_{b\Pi} &= C^2(1, 2, 1; 1, 0, 1) \bar{C}_b = \frac{1}{10} \bar{C}_b, \end{aligned} \quad (4.15a)$$

and

$$\bar{C}_b = \frac{32\pi^2}{9\hbar\omega_{D_b I}} |\langle D_b 1 || V^{(2)}(1,1) || I1 \rangle|^2 \quad (4.15b)$$

[see Fig. 6(b)]. From Eqs. (4.13) and (3.9) it follows that the  $B(\Lambda_I, M_{\Lambda_I}, J_I)$  in Eq. (4.10) are all equal to unity. From Eq. (4.10), one obtains an excitation cross section

$$\begin{aligned} \sigma'_{k'q'}(2, b) = & \frac{-32\pi^4(\hbar\omega_{ID_b})^{-2}}{9\hbar^3/2v_r|\bar{C}_b|^{1/2}|\Delta|^{1/2}} (\frac{1}{3})(\frac{1}{9}) \\ & \times |\langle D_b 1 || V^{(2)}(1,1) || I1 \rangle|^2 \\ & \times |\langle D_b 1 || \mu' || F2 \rangle|^2 \begin{Bmatrix} 4 \\ \sqrt{10} \end{Bmatrix} G_{k'q'} \begin{Bmatrix} 1 & 2 & 1 \\ 2 & 1 & k' \end{Bmatrix}. \end{aligned} \quad (4.16)$$

*Excitation scheme b:*  $j_i=j_{i'}=1, j_d=j_{d'}=0, j_f=0, j_{f'}=1$ . For this level scheme  $J_I=0, 1, 2$ ; however, since  $J_D=0$ , it follows from Eqs. (4.6) and (4.1) that only the state with  $J_I=2, M_I=0$  has its energy modified to second order in  $H_c(R)$ . Thus, to this order, the energies of the remaining eight states are not perturbed by the collisional interaction and those states do not contribute to the LICET cross section [Fig. 6(c)]. The energy level associated with state  $|I, \Lambda, M_{\Lambda}; t_e \rangle^{(0)} \simeq |I, J_I=2, M_I=0; t_e \rangle$  is given by

$$\Lambda(R, b) = I - C_b / R^6, \quad (4.17a)$$

where

$$C_b = \frac{32\pi^2}{3\hbar\omega_{D_b I}} |\langle I2 || V^{(2)}(1,1) || D_b 0 \rangle|^2. \quad (4.17b)$$

The excitation cross section evaluated from Eq. (4.10) is

$$\begin{aligned} \sigma'_{k'q'}(1,b) &= \frac{-32\pi^4(\hbar\omega_{ID_b})^{-2}}{9\hbar^{3/2}v_r|C_b|^{1/2}|\Delta|^{1/2}} \left(\frac{1}{9}\right) \\ &\times |\langle D_b 0 || V^{(2)}(1,1) || I2 \rangle|^2 |\langle D_b 0 || \mu' || F1 \rangle|^2 \\ &\times \left(\frac{1}{3}\right) (-1)^{k'} G_{k'q'}. \end{aligned} \quad (4.18)$$

The factor  $\left(\frac{1}{9}\right)$  represents the fact that only one of the nine states in the initial-state manifold contributes to the cross sections.

### B. Excitation schemes of Figs. 4(c) and 4(d)

For the excitation schemes of Figs. 4(c) and 4(d), the initial-state collisional interaction can be neglected. The eigenenergies are given by expressions analogous to those in Eqs. (2.19c) and (2.19d):

$$\Lambda_I(\alpha) = I, \quad (4.19)$$

$$\Lambda_F(R, \alpha) = F + \sum_{J_D M_D} \frac{|^{(0)}\langle F; t | H_c(\mathbf{R}(t)) | D_\alpha J_D M_D; t \rangle|^2}{\hbar\omega_{FD_\alpha}}, \quad \alpha = c, d.$$

The corresponding eigenkets are given by

$$\begin{aligned} |I; t_e; \alpha\rangle &\simeq |IJ_I M_I; t_e\rangle \\ |F; t_e; \alpha\rangle &\simeq |F; t_e\rangle^{(0)} + \sum_{J_D M_D} \frac{\langle D_\alpha J_D M_D; t_e | H_c(\mathbf{R}(t_e)) | F; t_e \rangle^{(0)}}{\hbar\omega_{FD_\alpha}} |D_\alpha J_D M_D; t_e\rangle, \quad \alpha = c, d. \end{aligned} \quad (4.20)$$

When Eqs. (4.19) and (4.20) are substituted into Eq. (3.5), it is possible to carry out the summation over  $M_I$ ,  $\tilde{M}$ , and  $\tilde{M}'$  to arrive at

$$\begin{aligned} \sigma_{KQ}^{J_F J'_F}(\alpha) &= 2N_I^{-1} (\hbar\omega_{FD_\alpha})^{-2} \\ &\times \sum_{R_e} \sum_{F, F', J_I} S_{\Lambda_F I}(R_e) G_{KQ} (2K+1)^{-1} (-1)^{J'_F - M'_F} C(J_F, J'_F, K; M_{\Lambda_F}, -M'_{\Lambda_F}, Q') \\ &\quad \times B(\Lambda_F, M_{\Lambda_F}, J_F) B^*(\Lambda_F, M'_{\Lambda_F}, J'_F) \langle d_{\tilde{Q}Q}^K(\varphi - \theta) \rangle \\ &\quad \times (-1)^{J_D - J'_D + J_I + M'_D} C(J_D, J'_D, K; M_D, -M'_D, \tilde{Q}) \\ &\quad \times \begin{Bmatrix} J_D & J'_D & K \\ 1 & 1 & J_I \end{Bmatrix} \langle D_\alpha J_D || \mu_T || IJ_I \rangle \langle D_\alpha J'_D || \mu_T || IJ_I \rangle^* \\ &\quad \times ^{(0)}\langle F; t_e | H_c(\mathbf{R}(t_e)) | D_\alpha J_D M_D; t_e \rangle \langle F'; t_e | H_c(\mathbf{R}(t_e)) | D_\alpha J'_D M'_D; t_e \rangle^* \delta_{\Lambda_F \Lambda'_F}, \end{aligned} \quad \alpha = c, d. \quad (4.21)$$

For the dipole-dipole interaction (4.1) and a final state with  $j_f = 0$ , Eqs. (4.1) and (4.4) can be used to reduce (4.21) to

$$\begin{aligned} \sigma'_{k'q'}(j_f, \alpha) &= \frac{64\pi^2}{3} N_I^{-1} (\hbar\omega_{FD_\alpha})^{-2} \\ &\times \sum_{R_e} \sum_{J_I, J_D, J'_D} S_{\Lambda_F I}(R_e) G_{k'q'} R_{\Lambda_F I}^{-6}(t_e) (2j_f + 1)^{-1} (-1)^{j_f + J_D - J'_D + J_I} (2k' + 1)^{-1} \\ &\quad \times \langle D_\alpha J_D || \mu_T || IJ_I \rangle \langle D_\alpha J'_D || \mu_T || IJ_I \rangle^* \langle Fj_f || V^{(2)}(1,1) || D_\alpha J_D \rangle \langle Fj_f || V^{(2)}(1,1) || D_\alpha J'_D \rangle^* \\ &\quad \times \langle d_{\tilde{Q}Q}^{k'}(\varphi - \theta) \rangle \begin{Bmatrix} J_D & J'_D & k' \\ 1 & 1 & J_I \end{Bmatrix} C(j_f, j_f, k'; M, -M', Q) \\ &\quad \times C(J_D, J'_D, k'; M, -M', Q) C(J_D, 2, j_f; M, 0, M) \\ &\quad \times C(J'_D, 2, j_f; M', 0, M') \delta_{|M||M'|}, \quad \alpha = c, d. \end{aligned} \quad (4.22)$$

The  $\delta$  function reflects the neglect of contributions resulting from the interference of different excitation channels.

*Excitation scheme c:*  $j_i=j_{i'}=0$ ,  $j_d=1$ ,  $j_{d'}=0$ ,  $j_{f'}=1$ . For this level scheme,  $J_I=0$ ,  $J_D=1$ . The final-state eigenkets to zeroth order are given by

$$\begin{aligned} |F; \Sigma, 0; t_e \rangle^{(0)} &= |F; j_{f'}=1, 0; t_e \rangle, \\ |F; \Pi, \pm 1; t_e \rangle^{(0)} &= |F; j_{f'}=1, \pm 1; t_e \rangle, \end{aligned} \quad (4.23)$$

and the corresponding eigenenergies from Eqs. (4.19) and (4.1) are

$$\begin{aligned} \Lambda_{\Sigma}(R, c) &= F - C_{c\Sigma}/R^6, \\ \Lambda_{\Pi}(R, c) &= F - C_{c\Pi}/R^6, \end{aligned} \quad (4.24)$$

where

$$\begin{aligned} C_{c\Sigma} &= \bar{C}_c C^2(1, 2, 1; 0, 0, 0), \\ C_{c\Pi} &= \bar{C}_c C^2(1, 2, 1; 1, 0, 1) \end{aligned} \quad (4.25a)$$

and

$$\bar{C}_c = \frac{32\pi^2}{9\hbar\omega_{D_c F}} |\langle D_c 1 || V^{(2)}(1, 1) || F 1 \rangle|^2 \quad (4.25b)$$

[see Fig. 6(d)]. The excitation cross section, calculated from Eqs. (4.22), (4.23)–(4.25), (4.6), (4.4), (4.1), and (4.12), is given by

$$\begin{aligned} \sigma'_{k'q'}(1, c) &= \frac{32\pi^4(\hbar\omega_{FD_c})^{-2}}{9\hbar^3/2v_r |\bar{C}_c|^{1/2} |\Delta|^{1/2}} \left(\frac{1}{9}\right) \\ &\times |\langle D_c 1 || \mu || I 0 \rangle|^2 \\ &\times |\langle F 1 || V^{(2)}(1, 1) || D_c 1 \rangle|^2 g_{k'q'}^c \end{aligned} \quad (4.26a)$$

where

$$\begin{aligned} g_{k'q'}^c &= -G_{k'q'} (-1)^{k'} (2k'+1)^{-1} \\ &\times \sum_Q \langle d_{QQ}^{k'}(\varphi - \theta) \rangle \\ &\times [C^2(1, 1, k'; 0, 0, Q) | C(1, 2, 1; 0, 0, 0) | \\ &\quad + 2C^2(1, 1, k'; 1, -1, Q) | C(1, 2, 1; 1, 0, 1) |] . \end{aligned} \quad (4.26b)$$

In the next section, we will need values for  $g_{00}^c$  and  $g_{20}^c$ . Those are given by

$$g_{00}^c = -G_{00} \left[ \frac{4}{3\sqrt{10}} \right], \quad (4.27a)$$

$$g_{20}^c = -\frac{G_{20}}{\sqrt{10}} \left[ \frac{1}{3} \langle d_{00}^2(\varphi - \theta) \rangle + \frac{2}{5} \langle d_{22}^2(\varphi - \theta) \rangle \right], \quad (4.27b)$$

where the relationship  $d_{00}^0(\theta)=1$  has been used. The value of  $g_{20}^c$  depends on the manner in which the decoupling angle  $\varphi$  is chosen.

*Excitation scheme d:*  $j_i=1$ ,  $j_{i'}=0$ ,  $j_d=j_{d'}=1$ ,  $j_f=0$ ,  $j_{f'}=2$ . For this level scheme  $J_I=1$ ,  $J_D=0, 1, 2, \dots$ , and  $J_F=2$ . The zeroth-order final-state eigenkets can be obtained from (4.3) as

$$\begin{aligned} |F; \Sigma, 0; t_e \rangle^{(0)} &= |F; J_F=2, M_F=0; t_e \rangle, \\ |F; \Pi, \pm 1; t_e \rangle^{(0)} &= |F; J_F=2, M_F=\pm 1; t_e \rangle, \\ |F; \Delta, \pm 2; t_e \rangle^{(0)} &= |F; J_F=2, M_F=\pm 2; t_e \rangle, \end{aligned} \quad (4.28)$$

along with the corresponding eigenenergies, obtained from (4.19) and (4.1),

$$\begin{aligned} \Lambda_{\Sigma}(R, d) &= F - C_{d0}/R^6, \\ \Lambda_{\Pi}(R, d) &= F - C_{d1}/R^6, \\ \Lambda_{\Delta}(R, d) &= F - C_{d2}/R^6, \end{aligned} \quad (4.29)$$

and

$$\begin{aligned} C_{dM} &= \frac{32\pi^2}{3\hbar\omega_{D_d F}} \sum_{J_D=0}^2 |\langle F 2 || V^{(2)}(1, 1) || D_d J_D \rangle|^2 \\ &\times C^2(J_D, 2, 2; M, 0, M), \quad M=0, \pm 1 \end{aligned} \quad (4.30)$$

[see Fig. 6(e)]. The  $C_{dM}$  can be expressed in terms of reduced matrix elements of atoms  $A$  and  $A'$  using (4.2) and simple properties of reduced matrix elements.<sup>17</sup> One finds

$$C_{dM} = C_d \Gamma_M, \quad (4.31)$$

where

$$\begin{aligned} C_d &= \frac{32\pi^2}{3\hbar\omega_{D_d F}} \left(\frac{5}{3}\right) |\langle f 0 || T^{(1)}(A) || d 1 \rangle|^2 \\ &\times |\langle f' 2 || T^{(1)}(A') || d' 1 \rangle|^2 \end{aligned} \quad (4.31b)$$

and

$$\Gamma_M = \sum_{J=0}^2 (2J+1) \begin{Bmatrix} 1 & 1 & J \\ 2 & 2 & 1 \end{Bmatrix}^2 C^2(J, 2, 2; M, 0, M), \quad (4.31c)$$

such that

$$\Gamma_0 = \frac{1}{10}, \quad \Gamma_1 = \frac{1}{12}, \quad \Gamma_2 = \frac{1}{30}. \quad (4.31d)$$

The cross section is obtained from Eq. (4.22). Expressed in terms of reduced matrix elements for the individual atoms,<sup>17</sup> this cross section is given by

$$\sigma'_{k'q'}(2, d) = \frac{32\pi^4(\hbar\omega_{FD_d})^{-2}}{9\hbar^3/2v_r |C_d|^{1/2} |\Delta|^{1/2}} \left(\frac{1}{3}\right) \left(\frac{1}{9}\right) |\langle f 0 || T^{(1)}(A) || d 0 \rangle|^2 |\langle f' 2 || T^{(1)}(A') || d' 1 \rangle|^2 |\langle d' 1 || \mu' || i' 0 \rangle|^2 g_{k'q'}^d, \quad (4.32)$$

where

$$\begin{aligned}
g_{k'q'}^d = & -(2k'+1)^{-1} G_{k'q'} \sum_{J_D, J_D'} (2J_D+1)(2J_D'+1) \begin{Bmatrix} 1 & 1 & J_D \\ 2 & 2 & 1 \end{Bmatrix} \begin{Bmatrix} 1 & 1 & J_D' \\ 2 & 2 & 1 \end{Bmatrix} \\
& \times \begin{Bmatrix} J_D & J_D' & k' \\ 1 & 1 & 1 \end{Bmatrix} \sum_{M, M', Q} |\Gamma_M|^{-1/2} \langle d_{\hat{Q}Q}^{k'}(\varphi-\theta) \rangle C(2, 2, k'; M, -M', Q) \\
& \times C(J_D, J_D', k'; M, -M', Q) C(J_D, 2, 2; M, 0, M) \\
& \times C(J_D', 2, 2; M', 0, M') \delta_{|M||M'|} \quad (4.33)
\end{aligned}$$

and  $\Gamma_M$  is given by (4.31c). When the summations are carried out for  $g_{00}^d$  and  $g_{20}^d$ , one finds

$$g_{00}^d = -0.325 G_{00}, \quad (4.34)$$

$$g_{20}^d = -[0.0339 \langle d_{00}^2(\varphi-\theta) \rangle + 0.0605 \langle d_{22}^2(\varphi-\theta) \rangle] G_{20}.$$

*Excitation scheme d:*  $j_i=j_i'=1$ ,  $j_d=1$ ,  $j_{d'}=0$ ,  $j_f=0$ ,  $j_{f'}=1$ . For this excitation scheme  $J_I=0, 1, 2$ ,  $J_D=1$ , and  $J_F=1$ . Final-state eigenkets and eigenenergies are the same as those given in Eqs. (4.23)–(4.25) with  $\tilde{C}_c$  replaced by

$$\tilde{C}_d = \frac{32\pi^2}{9\hbar\omega_{D_d F}} |\langle D_d 1 || V^{(2)}(1, 1) | F 1 \rangle|^2. \quad (4.35)$$

The excitation cross sections are obtained from Eq. (4.22). If the dipole-moment reduced matrix elements are expressed in terms of reduced matrix elements of atoms  $A$  and  $A'$ , then the sum over  $J_I$  can be carried out and one obtains

$$\begin{aligned}
\sigma'_{k'q'}(1, d) = & \frac{32\pi^4 (\hbar\omega_{FD_d})^{-2}}{9\hbar^3 v_r |\tilde{C}_d|^{1/2} |\Delta|^{1/2}} \\
& \times \left(\frac{1}{9}\right) \left(\frac{1}{3}\right) |\langle d'0 || \mu' || i'1 \rangle|^2 \\
& \times |\langle F 1 || V^{(2)}(1, 1) || D 1 \rangle|^2 g^d \delta_{k'0} \delta_{q'0} \quad (4.36a)
\end{aligned}$$

where

$$\begin{aligned}
g^d = & -G_{00} \sum_M C^2(1, 1, 0; M, -M, 0) |C(1, 2, 1; M, 0, M)| \\
= & -\frac{4}{3\sqrt{10}} G_{00}. \quad (4.36b)
\end{aligned}$$

The excitation scheme is shown in Fig. 6(f).

## V. DISCUSSION

General expressions for CARE (collisionally-aided radiative excitation) and LICET (light-induced collisional energy transfer) cross sections have been derived. The method of stationary phase was used to calculate LICET cross sections for detunings in the quasistatic wing of the excitation profile. As in CARE, the LICET cross sections depend on the slope of the interatomic potential

$d\omega_{FI}(R)/dR$  at the times of excitation. This feature has been exploited in CARE to obtain information on the difference between initial- and final-state interatomic potentials. The sensitivity of the analysis of CARE is enhanced significantly when one monitors the final-state magnetic polarization in addition to the total final-state population.

In practice, the use of LICET experiments to map out the interatomic potential is somewhat more restrictive. All LICET experiments have made use of a nearly resonant intermediate-state manifold to enhance the LICET cross sections. As such, the dominant collisional interaction is between this intermediate-state manifold and either the initial-state [excitation schemes of Figs. 4(a) and 4(b)] or the final-state [excitation schemes of Figs. 4(c) and 4(d)] manifold. Consequently, in contrast to CARE, the collisional interaction in LICET significantly modifies either the initial-state energies or final-state energies, but not both. Moreover, since the collisional interaction is nearly resonant, a single multipole term in this interatomic potential usually provides the major contribution to the collisional interaction (for the examples of Sec. IV, it was assumed that the dipole-dipole interactions produced the dominant contribution). Owing to this feature, the quasistatic wing of LICET profiles employing a nearly resonant intermediate state probes only the long-range part of the collisional interaction represented by the dominant multipole.

The final-state magnetic polarization can be monitored by fluorescence. As discussed in Sec. III, one measures the ratio

$$P = \frac{S_z - S_x}{S_z + S_x} \quad (5.1)$$

for radiation incident in the  $y$ -direction and polarized in the  $z$  direction. The quantities  $S_\beta(\beta=x, z)$  are the intensity of fluorescence polarized in the  $\beta$  direction. The fluorescence can be monitored on a transition from state  $f'$  to  $g'$  in atom  $A'$ . For incident radiation polarized in the  $z$  direction, the  $G_{k'q'}$  defined by (3.7) are equal to

$$G_{k'q'} = \left[ -\frac{1}{\sqrt{3}} \delta_{k'0} + \left[ \frac{2}{3} \right]^{1/2} \delta_{k'2} \right] |\mathcal{E}_0|^2 \delta_{q'0} \quad (5.2)$$

and the polarization ratio  $P$  is equal to<sup>9,18</sup>

$$P(\Delta) = 3 \left[ \frac{2\sqrt{6}(-1)^{j_{f'}+j_{g'}}}{3(2j_{f'}+1)^{1/2}} \begin{Bmatrix} 1 & 1 & 2 \\ j_{f'} & j_{f'} & j_{g'} \end{Bmatrix}^{-1} \frac{\sigma'_{00}(j_{f'})}{\sigma'_{20}(j_{f'})} + 1 \right]^{-1} \quad (5.3)$$

The polarization ratio  $P$  depends critically on which of the excitation schemes of Fig. 4 is used.

#### A. Excitation schemes of Figs. 4(a) and 4(b)

There is no depolarization following excitation so that all polarization information is produced at the time of excitation. Had we started from a *polarized* initial state, there would have been initial-state depolarization up to the time of excitation; since we consider only initially unpolarized states, they remain unpolarized up to the time of excitation. The final-state polarization produced in these excitation schemes is closely related to the impact limit result neglecting reorientation following excitation. The two results can be shown to lead to identical polarization rates for excitation scheme *a* if  $J_f=0$  or if the intermediate state  $|D\rangle = |dd'\rangle$  has either  $j_d=0$  or  $j_{d'}=0$  (if several  $J_D$  enter the calculation the polarization rates can differ); for excitation scheme *b* the polarization ratios are identical, independent of the values of the various angular momenta. All the specific cases studied in Sec. IV for excitation schemes *a* and *b* give rise to polarization ratios which are the same as those calculated in the impact limit neglecting depolarization following excitation.<sup>9</sup>

These *detuning-independent* polarization ratios are as follows.

*Excitation scheme a:*  $j_i=j_{i'}=0$ ;  $j_d=j_{d'}=1$ ,  $j_f=0$ ,  $j_{f'}=1$ ,  $j_{g'}=0$ . From Eqs. (4.12), (5.2), and (5.3), one finds

$$\frac{\sigma'_{00}(1,a)}{\sigma'_{20}(1,a)} = -\frac{10}{\sqrt{2}}, \quad P_a = \frac{1}{7}. \quad (5.4)$$

*Excitation scheme b:*  $j_i=1$ ,  $j_{i'}=0$ ,  $j_d=0$ ,  $j_{d'}=1$ ,  $j_f=0$ ,  $j_{f'}=2$ ,  $j_{g'}=1$ . From Eqs. (4.16), (5.2), and (5.3), one finds

$$\frac{\sigma'_{00}(2,b)}{\sigma'_{20}(2,b)} = -\frac{10}{\sqrt{70}}, \quad P_b = \frac{21}{47}. \quad (5.5)$$

This is the excitation scheme used by Débarre<sup>11</sup> in a LICET experiment with Eu "A" atoms and Sr "A'" atoms. She obtained a depolarization ratio  $P=0.43\pm 0.05$  independent of detuning in excellent agreement with (5.5) ( $\frac{21}{47}=0.47$ ).<sup>19</sup>

*Excitation scheme b:*  $j_i=j_{i'}=1$ ,  $j_d=j_{d'}=0$ ,  $j_f=0$ ,  $j_{f'}=1$ ,  $j_{g'}=0$ . From Eqs. (4.18), (5.2), and (5.3), one finds

$$\frac{\sigma'_{00}(1,b)}{\sigma'_{20}(1,b)} = -\frac{1}{\sqrt{2}}, \quad P_b = 1. \quad (5.6)$$

The physical significance of these polarization ratios has been discussed previously.<sup>9</sup>

#### B. Excitation schemes of Figs. 4(c) and 4(d)

The depolarization ratio now depends on  $\langle d_{QQ}^k(\varphi-\theta) \rangle$ . In terms of the impact parameter  $b$  of a collision, the angle  $\theta$  is defined by

$$\cos\theta = \frac{b}{R_e} \quad (5.7a)$$

and the angle  $\varphi$  by

$$\cos\varphi = \frac{b}{R_w}, \quad (5.7b)$$

where  $-\pi/2 \leq \theta \leq \pi/2$ ,  $-\pi/2 \leq \varphi \leq 0$ , and  $R_w$  is the decoupling radius. Equation (5.7) implies that

$$\cos\varphi = \frac{R_e}{R_w} \cos\theta. \quad (5.8)$$

Since  $R_e$  is a function of detuning  $\Delta$  through Eqs. (2.1) and (3.4), the cross sections and polarization ratio acquire a detuning dependence from the  $\langle d_{QQ}^k(\varphi-\theta) \rangle$  terms. It is not difficult to carry out the average (3.10) using (5.8). However, we can get an idea of the range of possible polarizations by considering the two extreme limits  $\varphi=\theta$  (no depolarization following excitation) to  $\varphi=\pi/2$  (depolarization out to  $R=\infty$  following excitation). Of course, the cross sections were derived assuming a finite  $R_w$  with no depolarization for  $R > R_w$ , but taking  $\varphi=\pi/2$  ( $R_w \sim \infty$ ) gives a lower bound for the polarization ratio.

The values of  $\langle d_{QQ}^k(\varphi-\theta) \rangle$  needed to evaluate the polarization ratios obtained from (3.10), are

$$d_{QQ}^k(0)=1, \quad d_{00}^0(\theta)=1, \quad \left\langle d_{00}^2 \left[ \frac{\pi}{2} - \theta \right] \right\rangle = 0, \quad (5.9)$$

$$\left\langle d_{22}^2 \left[ \frac{\pi}{2} - \theta \right] \right\rangle = \frac{1}{3}.$$

*Excitation scheme c:*  $j_i=j_{i'}=0$ ,  $j_d=1$ ,  $j_{d'}=0$ ,  $j_f=0$ ,  $j_{f'}=1$ ,  $j_{g'}=0$ . From Eqs. (4.26), (4.27), (5.2), (5.3), and (5.9), one finds

$$\frac{\sigma'_{00}(1,c)}{\sigma'_{20}(1,c)} = \begin{cases} -\frac{20}{11\sqrt{2}} & (\varphi=\theta) \\ -\frac{10}{\sqrt{2}} & (\varphi=\pi/2), \end{cases} \quad (5.10a)$$

$$P_c = \begin{cases} \frac{33}{51} & (\varphi=\theta) \\ \frac{1}{7} & (\varphi=\pi/2). \end{cases} \quad (5.10b)$$

For this level scheme, it is possible to show that the LICET polarization ratio is identical to that for a  $j'=0 \rightarrow 1$  CARE reaction.<sup>20</sup> The values of  $P_c$  in Eq. (5.10b) are identical to those calculated previously<sup>13,21</sup> for CARE for the same values of  $\varphi$ . This level scheme is also implicitly the one considered by Julienne<sup>10</sup> in modeling a LICET reaction. In the quasistatic wing, he found the same polarization ratio as for CARE excitation of a  $0 \rightarrow 1$  transition.

*Excitation scheme d:*  $j_i=1$ ,  $j_{i'}=0$ ,  $j_d=j_{d'}=1$ ,  $j_f=0$ ,  $j_{f'}=2$ ,  $j_{g'}=1$ . From Eqs. (4.33), (4.34), (5.2), (5.3), and (5.9), one finds

$$\frac{\sigma'_{00}(2,d)}{\sigma'_{20}(2,d)} = \begin{cases} -3.44/\sqrt{2} & (\varphi=\theta) \\ -16.1/\sqrt{2} & (\varphi=\pi/2) \end{cases}, \quad (5.11a)$$

$$P_d = \begin{cases} 0.237 & (\varphi=\theta) \\ 0.0541 & (\varphi=\pi/2) \end{cases}. \quad (5.11b)$$

Note that this is *not* the same polarization produced in a  $j'=1 \rightarrow 2$  CARE reaction.

*Excitation scheme d:*  $j_i=j_{i'}=1$ ,  $j_d=1$ ,  $j_{d'}=0$ ,  $j_f=0$ ,  $j_{f'}=1$ ,  $j_g=0$ . From Eqs. (4.36), (4.2), (5.3), and (5.9), one finds

$$\frac{\sigma'_{00}(1,d)}{\sigma'_{20}(1,d)} \sim \infty, \quad P_d=0. \quad (5.12)$$

As discussed previously,<sup>9</sup> excitation occurs from an inter-

mediate state having  $j_{d'}=0$ . In this case, it is the collisional interaction that produces the intermediate to final-state excitation [Fig. 4(d)]. The collision acts as an unpolarized field incident from all directions on atom  $A'$ ; consequently it produces an unpolarized final state in atom  $A'$ .

#### ACKNOWLEDGMENTS

This research was supported, in part, by National Science Foundation International Grant Nos. INT 8413300 and INT 8815036. The research of P.R.B. is supported by the U.S. Office of Naval Research. F.S. and G.N. acknowledge a travel allowance granted by the Netherlands Organization for the Advancement of Research (NWO) and the Centre National de la Recherche Scientifique (CNRS).

<sup>1</sup>V. S. Lisitsa and S. I. Yakovlenko, Zh. Eksp. Teor. Fiz. **66**, 1550 (1974) [Sov. Phys.—JETP **39**, 759 (1974)].

<sup>2</sup>S. Yeh and P. R. Berman, Phys. Rev. A **19**, 1106 (1979).

<sup>3</sup>L. I. Gudzenko and S. I. Yakovlenko, Zh. Eksp. Teor. Fiz. **62**, 1686 (1972) [Sov. Phys.—JETP **35**, 877 (1972)].

<sup>4</sup>Ph. Cahuzac and P. E. Toschek, Phys. Rev. Lett. **40**, 1087 (1978).

<sup>5</sup>For reviews of CARE and LICET containing additional references, see the following articles: S. I. Yakovlenko, Kvant. Elektron. (Moscow) **5**, 259 (1978) [Sov. J. Quantum Electron. **8**, 151 (1978)]; S. Yeh and P. R. Berman, Ref. 2; M. G. Payne, V. E. Anderson, and J. E. Turner, Phys. Rev. A **20**, 1032 (1979); P. R. Berman and E. J. Robinson, in *Photon-Assisted Collisions and Related Topics*, edited by N. K. Rahman and C. Guidotti (Harwood, Chur, Switzerland, 1982), pp. 15–33; P. R. Berman, J. Phys. (Paris) **46**, C1-11 (1985).

<sup>6</sup>For examples of CARE experiments, see J. L. Carlsten, A. Szöke, and M. G. Raymer, Phys. Rev. A **15**, 1029 (1977); A. Corney and J. V. M. McGinley, J. Phys. B **14**, 3047 (1981); W. J. Alford, N. Andersen, K. Burnett, and J. Cooper, Phys. Rev. A **30**, 2366 (1984), and references therein; K. Niemax, Phys. Rev. Lett. **55**, 56 (1985). The first LICET experiments were those of Falcone *et al.* [R. W. Falcone, W. R. Green, J. C. White, J. F. Young, and S. E. Harris, Phys. Rev. A **15**, 1333 (1977)], Cahuzac and Toschek (Ref. 4), C. Bréchnignac, Ph. Cahuzac, and P. E. Toschek, Phys. Rev. A **21**, 1969 (1980). The first several years of LICET experiments are reviewed in S. E. Harris, J. F. Young, R. W. Falcone, W. R. Green, D. B. Lidow, J. Lukasik, J. C. White, M. D. Wright, and G. A. Zdasiuk, in *Atomic Physics*, edited by D. Kleppner and F. M. Pipkin (Plenum, New York, 1981), pp. 407–428; somewhat more recent experiments are those of B. Cheron and S. Mosaddak, Opt. Commun. **54**, 7 (1985); F. Dorsch, S. Geltman, and P. E. Toschek, Phys. Rev. A **37**, 2441 (1988); M. Matera, M. Mazzoni, R. Buffa, S. Cavalieri, and E. Arimondo, Phys. Rev. A **36**, 1471 (1987).

<sup>7</sup>See, for example, J. Light and A. Szöke, Phys. Rev. A **18**, 1363 (1978); K. Burnett, J. Cooper, R. J. Ballagh, and E. W. Smith, *ibid.* **22**, 2005 (1980); K. Burnett and J. Cooper, *ibid.* **22**, 2027 (1980); **22**, 2044 (1980); E. L. Lewis, J. M. Salter, and M. Harris, J. Phys. B **14**, L173 (1981); E. L. Lewis, M. Harris, W.

J. Alford, J. Cooper, and K. Burnett, *ibid.* **16**, 553 (1983); J. Cooper, in *Spectral Line Shapes*, edited by K. Burnett (de Gruyter, Berlin, 1983), Vol. 2, p. 737; P. S. Julienne, *ibid.*, p. 769; G. Nienhuis, J. Phys. B **16**, 1 (1983); P. S. Julienne and F. H. Mies, Phys. Rev. A **30**, 831 (1984); F. H. Mies and P. S. Julienne, in *Spectral Line Shapes*, edited by F. Rostas (de Gruyter, Berlin, 1985), Vol. 3, p. 393; P. S. Julienne and F. H. Mies, Phys. Rev. A **34**, 3792 (1986); for a review of this area including both theory and experiment, see K. Burnett, Phys. Rep. **118**, 340 (1985); F. Schuller, G. Nienhuis, and W. Behmenburg, Z. Phys. D **2**, 193 (1986).

<sup>8</sup>See, for example, P. Thomann, K. Burnett, and J. Cooper, Phys. Rev. Lett. **45**, 1325 (1980); W. Behmenburg and V. Kroop, J. Phys. B **14**, 427 (1981); P. Thomann, K. Burnett, and J. Cooper, in *Spectral Line Shapes*, edited by B. Wende (de Gruyter, Berlin, 1981), Vol. 1, p. 929; W. J. Alford, N. Andersen, K. Burnett, and J. Cooper, Phys. Rev. A **30**, 2366 (1984); W. Behmenburg, V. Kroop, and F. Rebenrost, J. Phys. B **18**, 2693 (1985).

<sup>9</sup>P. R. Berman, Phys. Rev. A **22**, 1838 (1980); **22**, 1848 (1980); **29**, 2932 (1984).

<sup>10</sup>P. Julienne, in *Spectral Line Shapes*, edited by K. Burnett (de Gruyter, Berlin, 1983), Vol. 2, p. 769.

<sup>11</sup>A. Débarre, J. Phys. B **15**, 1693 (1982).

<sup>12</sup>To account for non-negligible population of state  $|D\rangle$  during the collision, a modified three-state theory of LICET has been developed. See A. Bambini and P. R. Berman, Phys. Rev. A **35**, 3753 (1987); A. Agresti, P. R. Berman, A. Bambini, and A. Stefanel, *ibid.* **38**, 2259 (1988); P. R. Berman, in *Atomic and Molecular Processes with Short Intense Laser Fields*, edited by A. D. Bandrauk (Plenum, New York, 1988), p. 75; P. R. Berman, in *Spectral Line Shapes*, edited by J. Szudy (Ossolineum, Wroclaw, 1989), Vol. 5, p. 713.

<sup>13</sup>J. Cooper in Ref. 7, p. 737. In this paper, the role of interference between different excitation channels is discussed.

<sup>14</sup>J. L. LeGouët and P. R. Berman, Phys. Rev. A **24**, 1831 (1982).

<sup>15</sup>L. I. Schiff, *Quantum Mechanics*, 3rd ed. (McGraw-Hill, New York, 1968), p. 250.

<sup>16</sup>P. R. Berman, Phys. Rev. A **29**, 957 (1984).

<sup>17</sup>All the necessary formulas can be found in the appendix of the

book by Messiah [A. Messiah, *Quantum Mechanics* (Wiley, New York, 1966), Vol. II]. In particular the Wigner-Eckart theorem is of the form  $\langle JM|T_{kq}|J'M'\rangle = (2J+1)^{-1}C(J',k,J;M',q,M)\langle J||T_k||J'\rangle$ .

<sup>18</sup>The polarization ratio is written assuming that there is no depolarization in subsequent collisions following excitation, before the fluorescence is monitored; that is, the collision rate times the lifetime of state  $g'$  is assumed to be much less than unity. Otherwise, the expression for  $P$  must be modified (see Refs. 7, 14, and 15).

<sup>19</sup>The Eu atoms have  $j_i = \frac{9}{2}$  and  $j_f = \frac{7}{2}$  which are different from the values assumed in the text; however, for excitation scheme  $b$  one can expand the reduced matrix elements to show that the  $k'q'$  dependence of  $\sigma'_{k'q'}(j_f, b)$  is given by

$$G_{k'q'} \begin{Bmatrix} j_f & j_f & k' \\ 1 & 1 & j_{d'} \end{Bmatrix},$$

independent of  $j_i$  and  $j_f$  (Ref. 9). Thus, the value of  $P = \frac{21}{47}$  is applicable to Débarre's experiment.

<sup>20</sup>By comparing the CARE and LICET cross sections for the LICET excitation scheme of Figs. 4(a) and 4(b), it is possible to show that they will yield the same polarization ratios provided that there is a single  $J_F$  and a single  $J_D$  which enter the LICET calculations; moreover, one must have  $J_D = J_F$ . The excitation scheme of Fig. 6(d) satisfied this requirement, but that of 6(e) does not.

<sup>21</sup>W. J. Alford, N. Andersen, K. Burnett, and J. Cooper, Ref. 8; P. S. Julienne and F. H. Mies, Ref. 7 (1986).